Comparative Analysis of Wrist-worn Energy Harvesting Architectures

R. Rantz[1], T. Xue[1], Q. Zhang[2], L. Gu[2], and K. Yang[2], S. Roundy[1]

[1]University of Utah, 1495 E 100 S (1550 MEK), Salt Lake City, UT 84112, USA
[2]Analog Devices, Inc., 804 Woburn St, Wilmington, MA 01887, USA

E-mail: robert.rantz@utah.edu

Abstract. This paper reports the simulation-based analysis of six dynamical structures with respect to their wrist-worn vibration energy harvesting capability. This work approaches the problem of maximizing energy harvesting potential at the wrist by considering multiple mechanical substructures independently of any specific transduction mechanism; rotational and linear motion-based architectures are considered. The addition of a linear spring element to the structures has the potential to improve power output. The analysis concludes that a sprung rotational harvester architecture outperforms a sprung linear architecture by 58% when real walking data is used as input to the simulations. The power output of a rotational prototype device was measured for various inputs and compared against simulation in order to corroborate the rotational device model.

1. Introduction

This paper reports the analysis of six dynamical structures with respect to their wrist-worn vibration energy harvesting capability. This work approaches the problem of maximizing energy harvesting potential at the wrist by considering multiple mechanical substructures independently of any specific transduction mechanism; this is accomplished by virtue of a modification to the standard Velocity Damped Resonant Generator (VDRG) model [1]. This approach serves as means to converge upon the device architecture that can best approach the theoretical maximum energy harvesting potential.

2. Structures

The first structure considered in the analysis is comprised of an eccentric seismic mass that rotates about an axis, as in [2]. Structure two is identical to structure one, except that a torsional spring acts on the mass, causing it to rest in the upper (with respect to gravity) semicircle when subject to no external input. See **Figure 1**. The third structure is a one-dimensional linear slide, comprised of a seismic mass that is free to move in a single dimension up to the length of the device where impact occurs. Structure four is structure three with a linear spring element. See Figure 2. Additionally, two-dimensional analogs of the third and fourth structures were considered that are composed of independent linear elements for the two available degrees of freedom, and a single seismic mass.

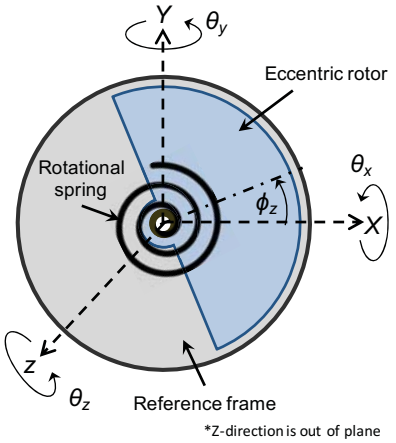

Figure 1. Rotational harvester architecture, pictured with a torsional spring (as in structure two).

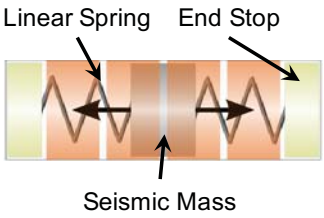

Figure 2. One-dimensional linear slide architecture, pictured with spring (as in structure four).

3. Comparative Analysis

Mathematical models of the various structures were used for simulations in order to determine the average power output of each architecture in response to various inputs. In all cases, the models assume that electrical power transduction may be modelled as an ideal viscous damper with a viscous damping coefficient (known henceforth as an electrical damping coefficient) to be determined via optimization. Power dissipated in the electrical damper is considered to be the power output of the architecture.

In the case of all structures, an arbitrary constraint of 1 cm^3 total device volume (as determined by the swept volume of the seismic mass as it is displaced through its full range of motion) is applied. The spring and damper structures are assumed to consume no volume.

The rotational structures made use of the system model described in [2], which was modified to include a rotational spring term for structure two.

The linear systems were assumed to be well-modeled as a base-excited mass spring damper system, as in the VDRG model [1], except that the seismic mass is displacement-limited, and contact with an end stop results in a reversal of velocity that is reduced via a coefficient of restitution. In the case of the unsprung architectures, the spring constant is assumed to be zero. Mechanical friction is modelled as viscous for all structures considered in the analysis.

3.1. Optimization. The value of the electrical damping coefficient and, in the case of architectures with springs, the spring constant greatly impact the nature of the dynamic response of a given architecture. For any particular input signal, the goal is to select values for the electrical damping coefficient and, when applicable, the spring constant such that maximum power is dissipated in the electrical damper. The power output of each structure may then be compared for a given input signal.

Because the input signals can be complex in nature and, in the case of structures one and two, the differential equation describing a structure highly nonlinear, a numerical Pattern Search (PS) algorithm was used in MATLAB to determine optimal system parameters for a given input signal [3]. An objective function was formed using the output of a numerical differential equations solver; the design parameters were the input to the objective function, and the output is the average power dissipated in the electrical damper over the duration of the input signal.

Some geometric optimization was performed on the linear structures. The additional design variables included the length and width of the swept volume, and the dimensions of the seismic mass.

3.2. *Inputs*. Two types of inputs were considered for the analysis. Firstly, a "pseudo-walking" input comprised of a single sinusoid derived from the motion of a driven pendulum that approximates the swing of a human arm during vigorous walking. Secondly, a collection of 6-axis inertial data collected from the wrists of five subjects during a casual walking motion. For the collection of real walking data, the optimal design parameters of each device were determined for each walking signal individually by virtue of the PS algorithm, and the maximum, minimum, and average power output of each signal found for every device architecture.

4. Model Validation

A rotational prototype device, representing a physical implementation of structure one, was constructed for the purpose of empirically validating the rotational model used in the analysis. See Figure 3.

An electromagnetic transducer was constructed for the purpose of measuring power output which consisted of an array of twenty magnets embedded in a dual-rotor design and ten corresponding circular planar copper coils. A load resistance which matched the 240 Ω coil resistance was placed across the output of the device and the voltage across the load was measured in order to compute average power dissipation. In order to reproduce a pseudo-walking input, a stepper motor-driven swing arm setup was constructed and was fed the appropriate angular position commands to reproduce the ideal signal. See Figure 4.

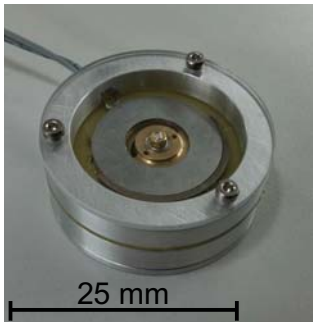

Figure 3. Rotational prototype device with an electromagnetic transducer.

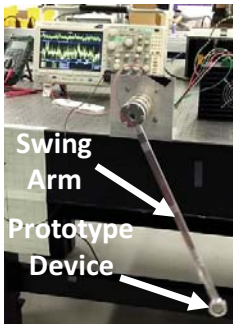

Figure 4. Swing arm experimental setup during operation.

The results of the experiment are summarized in Figure 5, which show general agreement between simulation and experimental measurement.

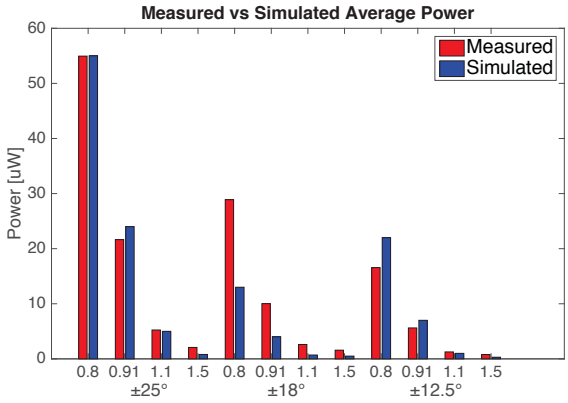

Figure 5. Comparison of measured vs simulated test data for pseudo-walking inputs. Three amplitudes and four periods were tested.

5. Results

The optimal geometry of the two-dimensional slide structures was found to converge to the optimal one-dimensional slide structure geometries for all provided inputs, indicating that the additional dimension does not provide any benefit in terms of power output. For this reason, the two dimensional linear structures (structures five and six) were no longer considered after the optimization step.

The addition of springs to all devices generally improved performance for both pseudo-walking and real walking data inputs in the simulation-based comparative analysis. In the case of sprung vs unsprung rotational harvesters (structures one and two), the addition of a spring improved performance by 365% under pseudo-walking input, and an average of 68% under real walking inputs. In the case of the linear slide structures (structures three and four), the addition of a spring did not significantly improve performance under pseudo-walking input, but improved performance by an average of 197% under real walking inputs. See Figure 6. The average power output of the sprung rotational architecture (structure two) was 58% greater than the average for the sprung linear slide (structure four) using real walking data as inputs. A consequence of adding a spring to the rotational structure is increased sensitivity of power output to electrical damping coefficient. See Figure 7.

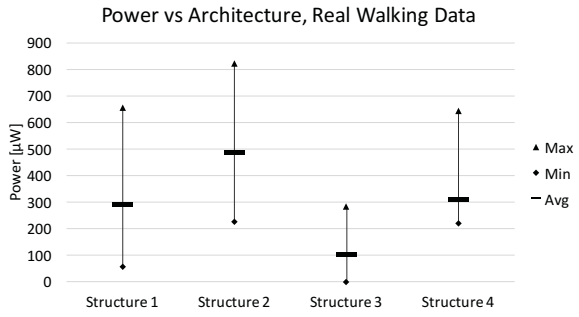

Figure 6. Maximum, minimum, and average power output of structures subject to five real walking data signals.

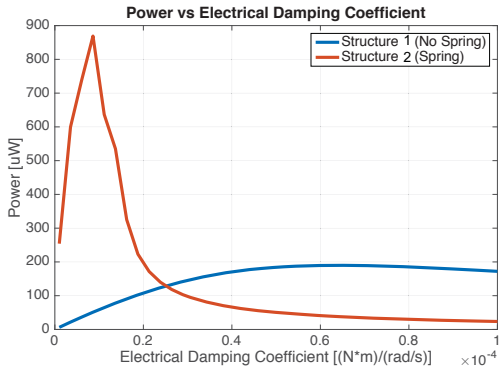

Figure 7. Power vs electrical damping coefficient for the two rotational structures. Notice sharp drop of power output when electrical damping constant is not near the optimal value.

6. Conclusions

A simulation-based comparative analysis of six vibration energy harvesting structures was performed. The addition of a spring to all structures considered in the study resulted in improved simulated power output for real walking data. The average power output of the sprung rotational structure was 58% greater than the average for the sprung linear slide using real walking data as inputs.

Acknowledgements

Funding for this research was provided by the National Science Foundation under Award Number ECCS 1342070, and a generous grant from Analog Devices Inc.

References

[1] P. Mitcheson, T. C. Green, E. M.Yeatman, and H. A. S., "Architectures For Vibration Driven Micropower Generators," *J. Microelectromechanic Syst.*, vol. 13, no. 3, pp. 429–440, 2004.

[2] T. Xue, X. Ma, C. Rahn, and S. Roundy, "Analysis of Upper Bound Power Output for a Wrist-Worn Rotational Energy Harvester from Real-World Measured Inputs," *J. Phys. Conf. Ser. 557 012090*, vol. 557, pp. 3–7, 2014.

[3] Mathworks, "Global Optimization Toolbox: User's Guide (R2016b)," 2016. [Online]. Available: http://www.mathworks.com/help/pdf_doc/gads/gads_tb.pdf. [Accessed: 15-Sep-2016].